Multi-Objective Topology Optimization and PID-Controlled Grasping of Compliant Fingers for Parallel Robotic Grippers

Gidugu Lakshmi Srinivas, Pataki Abel Endre, Hasanaj Dea, and Mathias Brandstötter

ADMiRE Research Center, Carinthia University of Applied Sciences,
Europastraße 4, Austria,
{l.gidugu,m.brandstoetter}@cuas.at,
WWW home page: http://www.admire.center

Abstract. Adaptive grasping of objects with varying geometry remains an important problem in robotic manipulation. Although compliant Fin-Ray-inspired fingers provide better passive adaptation than rigid grippers, the combined design of lightweight finger topology and controlled force interaction is still limited in many practical parallel gripper systems. This paper presents a topology-optimized compliant finger design together with a PID-based force control framework for a parallel robotic gripper. The finger was modeled with an inner triangular design region and an outer non-design frame, and density-based structural optimization was performed in ANSYS Workbench using the Sequential Convex Programming solver. The optimization objective combined maximization of directional deformation in the desired wrapping direction with minimization of equivalent von Mises stress, while a mass constraint of 15 g was imposed to match the reference Fin Ray finger. The structural model was analyzed under a fixed support at the mounting face and a distributed load of 10 N at the selected contact region. The optimized density result was subsequently reconstructed into a printable three-dimensional finger geometry using SpaceClaim with manufacturing-aware post-processing. In addition, a PID-based force control strategy was formulated using a second-order servo approximation and real-time force feedback from a SingleTact sensor. A dedicated experimental test bench was developed for comparative grasping tests. Grasping experiments were conducted using an orange at 10 N and 3D-printed cylinder and sphere objects at 5 N, with ten repeated trials for each condition. The optimized finger improved the wrapping angle by 9.5%, 12.3%, and 28.7% for the orange, cylinder, and sphere, respectively, compared with the reference Fin-Ray finger. The study provides a practical design, control, and validation workflow for compliant robotic fingers and demonstrates improved object-contact coverage for the optimized design under the tested grasping condition.

Keywords: Adaptive grasping · Compliant gripper · Fin-Ray finger · Force control · PID control · Topology optimization

S. Uppapalli and D. Chakraborty (eds.), *Proceedings of the International Conference on Mechanics, Materials and Mechatronics (ICM³ 2026)*, Atlantis Highlights in Engineering 47,
https://doi.org/10.2991/978-94-6239-764-4_16

1 Introduction

Robotic grasping is an important function in industrial automation, service robotics, and handling of delicate products. However, rigid grippers usually require accurate positioning and often show limited adaptability when the object shape, local stiffness, or contact condition changes. Bio-inspired soft robotics was introduced to address this limitation by using structural compliance for safer and more adaptive physical interaction [6]. The broader development of soft robots has shown that material compliance can support both safe contact and simplified mechanical behavior in manipulation tasks [7]. Reviews of soft manipulators and grippers further indicate that compliant gripping concepts are especially suitable for uncertain and fragile objects, where passive adaptation and larger contact area are required [3, 9].

Among compliant gripping concepts, the Fin-Ray effect has received significant attention because the finger bends toward the applied transverse load and wraps around the contacted object [2]. This behavior has been studied further through analytical and numerical models that explain how the finger geometry influences deformation and load transfer [8]. Fin-Ray-inspired grippers with embedded sensing and force feedback have also demonstrated improved grasp monitoring and safer interaction with the object [15]. More recent work on 3D-printed Fin-Ray fingers has shown that lightweight redesign can improve material efficiency while maintaining useful grasping behavior [12]. At the same time, structural studies have confirmed that wrapping performance is strongly affected by the internal rib arrangement and by the load case used during evaluation [13].

To improve such structures in a systematic manner, topology optimization provides a direct way to distribute material inside a prescribed design domain according to defined objectives and constraints [1]. Its application to compliant mechanism synthesis is well established, beginning with early topology optimization methods for compliant motion generation [10]. Later reviews have summarized the main continuum-based formulations and design objectives used for compliant structures [17]. In the context of Fin-Ray-inspired fingers, recent studies have considered multiple load cases, lightweight redesign, and multi-material adaptive layouts to improve grasping performance under different object-contact conditions [5, 11]. Related work has also shown that sensing-aware finger design is important when structural compliance and grasp-force estimation must be addressed together [16]. Soft robotics studies have shown that compliant structures improve safe and adaptive interaction in uncertain environments [14]. Related review work further highlighted the value of bio-inspired soft systems for grasping irregular objects and simplifying mechanical design in manipulation [4].

The main contributions of this paper are as follows. First, a manufacturable topology optimization workflow is presented for a compliant Fin-Ray-inspired finger using ANSYS Workbench with explicit design and non-design regions. Second, the optimized density result is converted into a printable 3D finger geometry through SpaceClaim-based design-to-manufacture reconstruction. Third, a PID-based force control framework is integrated with the compliant finger design and validated through preliminary grasping experiments on a real object.

2 Methodology

2.1 Topology optimization method

In this work, the conventional Fin Ray finger geometry was used as the starting reference for topology optimization. To define a manufacturable design problem, the original internal rectangular ribs were removed and replaced by a solid inner triangular region that served as the design domain. The outer triangular frame of the finger was preserved as a non-design region in order to maintain the original external envelope, contact contour, and mounting compatibility. In addition, the top mounting region associated with the screw connection and the local contact region corresponding to the object-touching surface were excluded from the design domain.

The optimization model was prepared in Rhino 8 and imported into ANSYS Workbench. A density-based topology optimization approach was then applied in the Structural Optimization module. The inner triangular core was defined as the design region, whereas the outer frame, the mounting zone, and the contact patch were treated as exclusion regions. The material redistribution was restricted to the interior of the finger while preserving the functional outer boundary.

A static structural analysis was first established to define the loading and boundary conditions. The finger was fixed at the upper mounting face, which represents the screw-supported connection to the gripper body. A distributed load was applied on the predefined contact patch located on the grasping side of the finger, corresponding to the region where the finger interacts with the object during grasping. This loading arrangement was selected to reproduce the deformation mode required for adaptive wrapping. The material interpolation in the topology optimization was represented using a density-based SIMP formulation, in which the elastic modulus of each element is expressed as

$$E_e(\rho_e) = E_{\min} + \rho_e^p \left(E_0 - E_{\min}\right), \tag{1}$$

where $\rho_e \in [\rho_{\min}, 1]$ is the elemental density variable, E_0 is the Young's modulus of the solid material, $E_{\min}$ is a small stiffness assigned to void-like elements to avoid numerical singularity, and p is the penalization factor. In the present work, a penalization factor of $p = 3$ was used. To promote a compliant response while avoiding excessive local stress, a multi-objective formulation was adopted. The first objective was defined as the maximization of the directional displacement at the contact region, specified in ANSYS through a primary criterion. The second objective was the minimization of the equivalent von Mises stress. Since the optimization algorithm operates in a minimization framework, the displacement objective was introduced with a negative sign. The normalized objective function can therefore be written as

$$\min_{\rho} \ J(\rho) = w_1 \left(-\frac{u_c(\rho)}{u_{c,0}}\right) + w_2 \left(\frac{\sigma_{\mathrm{vm}}(\rho)}{\sigma_{\mathrm{vm},0}}\right), \tag{2}$$

where u_c is the directional displacement at the selected contact region, σ_{vm} is the equivalent von Mises stress, $u_{c,0}$ and $\sigma_{\mathrm{vm},0}$ are the corresponding reference values obtained from the baseline design, and w_1 and w_2 are the weighting factors used in the normalized-sum objective definition. The optimization problem was subject to a mass constraint in order to ensure a fair comparison with the original Fin Ray finger. The constraint is expressed as

$$\frac{m(\rho)}{m_0} \leq 1, \tag{3}$$

where $m(\rho)$ is the mass of the optimized design and m_0 is the mass of the reference finger. In the present implementation, the weighting factors were selected as $w_1 = 0.70$ and $w_2 = 0.30$. A higher weight was assigned to the directional-displacement term because the main functional requirement of the finger is adaptive wrapping around the object. The stress term was retained with a lower but nonzero weight to avoid highly localized deformation and to maintain a structurally continuous printable load path. The same weighting values were used for all optimization runs reported in this work. In addition, the density variables satisfy

$$\rho_{\min} \leq \rho_e \leq 1. \tag{4}$$

The optimization was performed in ANSYS Workbench using the density-based topology optimization option with the Sequential Convex Programming solver. The optimization settings included a maximum iteration count of 500, a minimum normalized density of 10^{-3}, a convergence accuracy of 0.1%, and a program-controlled density filter. After completion of the optimization, the resulting density distribution was interpreted and converted into a smooth printable geometry. During this post-processing stage, disconnected features and very thin members were removed, sharp transitions were blended, and the final layout was rebuilt as a manufacturable solid model while preserving the non-design outer frame and mounting features.

2.2 PID-based force control and controller tuning

To achieve controlled grasping with compliant fingers, a PID-based force control strategy was implemented using real-time feedback from the SingleTact force sensor. The servo actuator was represented by a second-order approximation of its closed-loop position dynamics, which provides a practical model for controller design under small to medium motion conditions. Based on the manufacturer specification of a settling time of $T_s = 0.14\,\mathrm{s}$ for a 60° motion at 4.8 V, and assuming near-critical damping ($\zeta = 1$), the natural frequency was estimated as

$$\omega_n = \frac{4}{T_s} = \frac{4}{0.14} = 28.57\,\mathrm{rad/s}. \tag{5}$$

Accordingly, the servo dynamics were approximated by the transfer function

$$G(s) = \frac{\omega_n^2}{s^2 + 2\zeta\omega_n s + \omega_n^2} = \frac{816.24}{s^2 + 57.14s + 816.24}. \tag{6}$$

The gripping force was regulated by the PID control law

$$u(t) = K_p e(t) + K_i \int_0^t e(\tau)\,\mathrm{d}\tau + K_d \frac{\mathrm{d}e(t)}{\mathrm{d}t}, \tag{7}$$

where $u(t)$ is the control input to the servo actuator and

$$e(t) = F_{\mathrm{ref}}(t) - F_{\mathrm{m}}(t) \tag{8}$$

denotes the force tracking error between the reference gripping force F_{ref} and the measured force F_{m}.

The controller parameters were obtained in MATLAB using the `pidtune` function with a crossover frequency selected close to the identified natural frequency in order to achieve a stable and sufficiently fast response. The final controller gains were selected as

$$K_p = 1.5538, \qquad K_i = 32.7129, \qquad K_d = 0.018. \tag{9}$$

The measured force was calculated from the sensor output after zero-offset correction according to

$$F_{\mathrm{m}} = \frac{D - D_0}{512} F_{\mathrm{rated}}, \tag{10}$$

where D is the digital sensor output, D_0 is the baseline output obtained during calibration, and F_{rated} is the nominal force range of the sensor. The controller output was mapped to the admissible servo angle range, and the control loop was executed with a sampling period of 100 ms. This approach enabled direct regulation of the gripping force during object interaction while remaining suitable for implementation on the embedded control hardware.

2.3 Experimental setup

A dedicated experimental test bench was developed to evaluate the grasping behavior of the compliant fingers under controlled loading conditions, as shown in Fig. 1. The setup consists of two opposing grippers mounted on a spindle-driven mechanism that moves the fingers symmetrically toward the object. The supporting structure was assembled from modular aluminum profiles, while the mounting and connection components were fabricated by additive manufacturing to simplify alignment and replacement of the test fingers.

The force-control procedure used in the setup is summarized in Algorithm 1. At the beginning of each test, the communication interfaces, actuator, and force sensors were initialized. The force sensors were then calibrated to determine the zero-offset values before grasping. During operation, the sensor signals were read continuously, converted into force values, and used to compute the average gripping force. The PID controller then updated the actuator command until the predefined target force was achieved. In the present study, the setup was used to compare the reference Fin-Ray finger and the optimized finger using three test

Algorithm 1 Closed-loop force-controlled grasping procedure

```
Initialize actuator, controller, and communication interfaces
Calibrate force sensors and store zero-offset values
Set desired gripping force
while grasping test is active do
    Read force sensor signals
    Convert sensor readings into force values
    Compute the average gripping force
    Evaluate PID control law
    Update actuator motion
    if target gripping force is reached then
        Stop motion and capture grasping image
    end if
end while
```

objects: an orange, a 3D-printed cylinder, and a 3D-printed sphere. The orange was tested at 10 N, while the 3D-printed objects were tested at 5 N, and each grasping condition was repeated ten times. Grasping performance was assessed from front-view images by manually identifying the finger-object contact points and calculating the corresponding wrapping angles and contact arc lengths.

3 Results and discussions

3.1 Topologically optimized fingers

The structural optimization study was carried out in ANSYS using the finger model with TPC 40D material properties, a fixed support applied on the top mounting face, and a distributed compressive load of 10 N applied on the selected contact region, as shown in Fig. 2. The TPC 40D key material properties: density $\rho = 1.22$ g/cm^3, Young's modulus $E = 50$ MPa, Poisson's ratio $\nu = 0.45$, and tensile strength $\sigma_{\mathrm{t}} = 10$ MPa. The optimization problem was defined with a density-based topology formulation and solved using the Sequential Convex Programming algorithm. The inner triangular core of the finger was assigned as the design region, whereas the outer peripheral frame was retained as a non-design region in order to preserve the external grasping profile and the mounting interface. In the objective definition, the primary criterion was set to maximize the directional deformation in the desired wrapping direction, while the equivalent von Mises stress was simultaneously reduced through the secondary objective. A mass constraint of 15 g was imposed to match the mass of the reference Fin Ray finger, which corresponds to approximately 25% of the fully solid initial design space. The preliminary static structural results showed the stress distribution and deformation trend within the prescribed domain before material redistribution. Based on these conditions, the optimization generated a modified internal load path that improved compliance in the required direction while maintaining the outer frame. The resulting topology was then interpreted and reconstructed as a printable geometry for subsequent fabrication and validation.

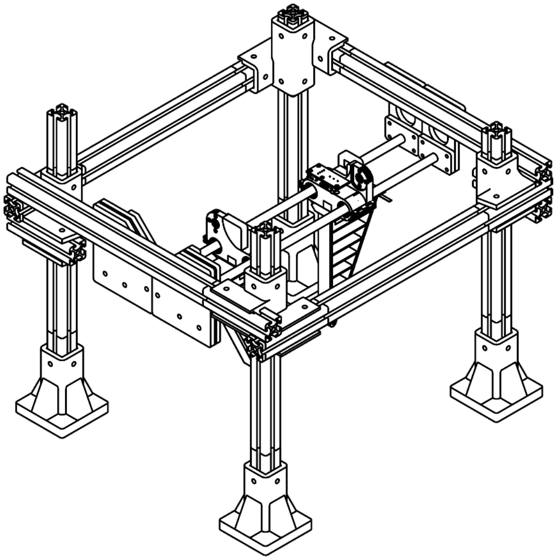

Fig. 1. Experimental setup for deformation analysis of soft fingers.

The converged 3D topology result from ANSYS was converted into a printable solid model through post-processing in SpaceClaim, as shown in Fig. 3. Manufacturing constraints applied during optimization were used to control the minimum structural feature size and to reduce the formation of unstable thin members. The resulting density field was interpreted to extract the principal material network responsible for load transfer between the mounting region and the contact region. Based on this distribution, the internal members were rebuilt as a continuous solid geometry, whereas disconnected low-density zones and geometrical details below the practical printing limit were removed. The reconstructed topology was then smoothed and locally edited to obtain continuous load paths, stable member junctions, and printable wall dimensions across the full 3D geometry. This design-to-manufacture step produced a fabrication-ready finger model without changing the main deformation mechanism predicted by the optimization.

3.2 Force regulation performance during grasping

The proposed PID-based force control strategy provided stable force regulation during grasping and supported controlled interaction between the compliant fingers and the target object. Based on the identified servo model, the tuned controller yielded a fast closed-loop response with limited overshoot, which is desirable for grasping tasks in which sudden force peaks should be avoided. In particular, the selected proportional gain provided sufficient responsiveness, while the integral gain improved compensation of steady-state deviations caused

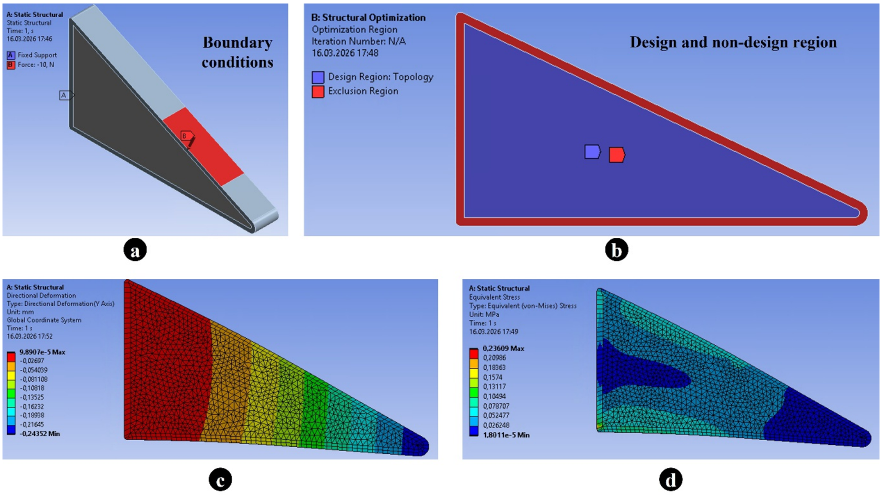

Fig. 2. Structural optimization setup and static structural response of the finger model: (a) boundary conditions, (b) design and non-design regions, (c) equivalent stress, and (d) directional deformation.

by compliance, friction, and transmission effects in the actuator-gripper system. The relatively small derivative gain was found to be appropriate for the present setup, since the measured force signal is affected by sensor noise and by the deformation of the soft structure. A larger derivative contribution would amplify these fluctuations and reduce the robustness of the control action. The selected gain combination therefore represents a practical compromise between response speed, stability, and noise sensitivity.

Figure 4 shows the closed-loop response of the tuned controller for a 5 N force command using the identified second-order servo approximation. The response reached the target without sustained oscillation. The peak force was approximately 5.30 N, corresponding to an overshoot of approximately 6.0%. The 2% settling time was approximately 0.20 s and the steady-state error was approximately 0.014 N. These values indicate that the controller is sufficiently fast for the quasi-static grasping experiments while avoiding excessive force overshoot.

The experimental setup further showed that force feedback is important for repeatable grasping of objects with varying geometry. In contrast to purely position-driven actuation, the proposed approach allows the gripper to adjust its motion according to the measured contact force and therefore maintain a more controlled gripping condition. This is especially relevant for compliant fingers, where structural deformation changes the contact state continuously during the grasping process. At the same time, the present results indicate several factors that influence the quality of force regulation. The sensor is positioned behind the direct contact region in order to maintain reliable contact during deformation, which may introduce a lever-arm effect in the measured force. In addition,

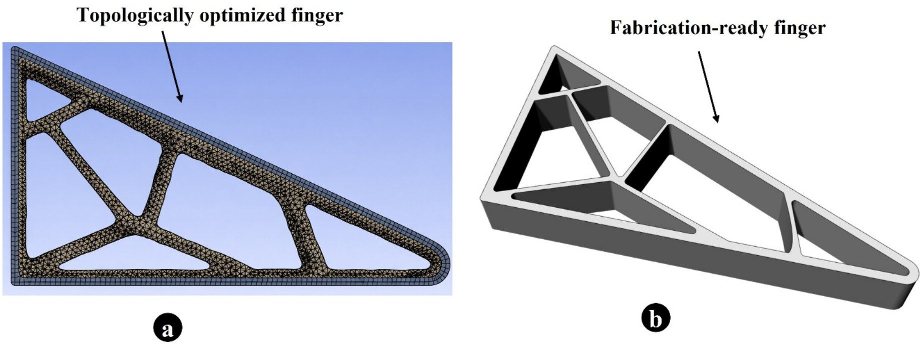

Fig. 3. Conversion of the optimized 3D topology result into a printable CAD model.

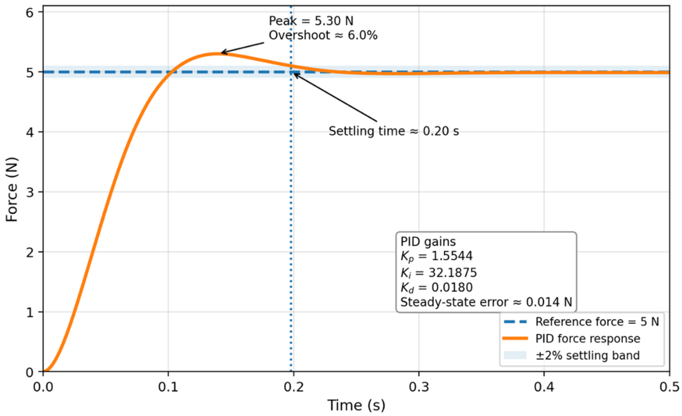

Fig. 4. Closed-loop PID force response for a 5 N grasping target.

the current image-based manual measurement procedure does not yet provide the desired level of accuracy and repeatability for detailed deformation analysis. Despite these limitations, the obtained results confirm that the proposed control approach is suitable for compliant parallel grippers and provides a sound basis for future refinement through improved calibration and additional sensing.

3.3 Demonstration of grasping tasks

The grasping performance of the reference Fin-Ray finger and the optimized finger was evaluated using three test objects: an orange, a 3D-printed cylinder, and a 3D-printed sphere. The orange was tested at a target gripping force of 10 N, whereas the 3D-printed cylinder and sphere were tested at 5 N. For each object, ten repeated trials were conducted. The wrapping behavior was quantified from front-view images by identifying the upper and lower contact points between the finger and the object and measuring the total contact angle with respect to the

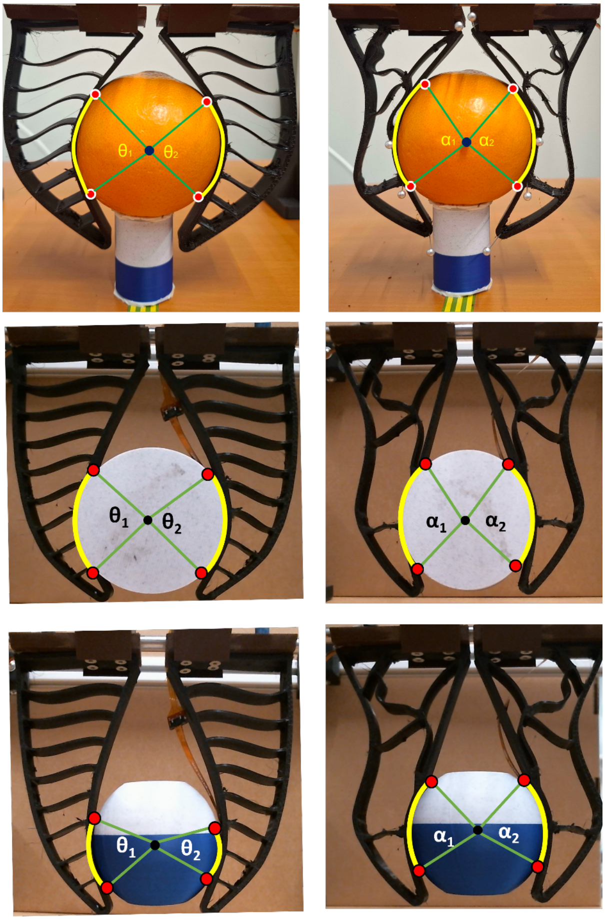

Fig. 5. Image-based comparison of grasping performance for the reference Fin-Ray finger and the optimized finger using an orange at 10 N and 3D-printed objects at 5 N.

object center, as shown in Fig. 5. The contact arc length was then calculated from the measured object diameter and the corresponding wrapping angle. The results are summarized in Table 1. For all tested objects, the optimized finger achieved a higher wrapping angle and a larger contact arc length than the reference Fin-Ray finger. The relative improvement in wrapping angle was 9.5% for the orange, 12.3% for the cylinder, and 28.7% for the sphere. These results show that the optimized internal topology improves object-conforming behavior under different grasping geometries and force conditions, while the small standard deviations indicate repeatable grasping performance across the repeated trials.

Future work will focus on extending the grasping evaluation through repeated and quantitative experiments under controlled loading conditions. In the next stage, both finger designs will be tested over multiple trials and on objects with

Table 1. Grasping performance of the Fin-Ray and optimized fingers over repeated trials.

Object	**F (N)**	**n**	ϕ_F **(deg)**	ϕ_O **(deg)**	**Gain (%)**	s_F **(mm)**	s_O **(mm)**
Orange	10	10	166.6 ± 1.4	182.5 ± 1.2	9.5	101.7 ± 0.9	111.4 ± 0.8
Cylinder	5	10	144.8 ± 1.4	162.6 ± 1.2	12.3	92.7 ± 0.9	100.9 ± 0.8
Sphere	5	10	73.5 ± 1.5	94.6 ± 1.3	28.7	87.6 ± 0.9	95.0 ± 0.8

F: target gripping force; ϕ_F: wrapping angle of the reference Fin-Ray finger; ϕ_O: wrapping angle of the optimized finger; s_F: contact arc length of the reference Fin-Ray finger; s_O: contact arc length of the optimized finger.

different diameters and stiffness in order to assess repeatability and sensitivity to object geometry. A computer-vision-based measurement approach will be developed to automatically extract contact angle, contact length, and marker displacement from calibrated image sequences. In addition, displacement sensing will be integrated into the setup to measure the maximum deformation of selected finger locations during grasping. These improvements will reduce manual measurement error, provide more consistent data processing, and enable a stronger correlation between force input, structural deformation, and grasping performance.

4 Conclusions

This paper presented a combined structural design and force-control framework for compliant fingers used in parallel robotic grippers. A density-based topology optimization method was implemented in ANSYS Workbench by defining an inner triangular design region and preserving the outer frame, mounting region, and contact region as non-design areas. Under a fixed support at the mounting face and a distributed load of 10 N at the contact region, the optimized layout was obtained using a multi-objective formulation based on directional deformation and equivalent stress, together with a mass constraint of 15 g to match the reference Fin Ray finger. The resulting topology was then converted into a printable three-dimensional geometry through manufacturability-oriented post-processing in SpaceClaim. A PID-based gripping-force control strategy was formulated using a second-order approximation of the servo dynamics and real-time force feedback from a SingleTact sensor. In addition, a dedicated test bench was developed to enable controlled comparison of the reference Fin Ray finger and the optimized finger under identical grasping conditions. Grasping experiments were carried out using an orange at 10 N and 3D-printed cylinder and sphere objects at 5 N. Across ten repeated trials, the optimized finger showed consistent improvement over the reference Fin-Ray finger, increasing the wrapping angle by 9.5%, 12.3%, and 28.7% for the orange, cylinder, and sphere, respectively. These preliminary results indicate that the optimized design provided greater object-contact coverage and improved wrapping behavior under the tested condition. Future work will focus on repeated grasping experiments, evaluation on objects with different geometry and stiffness, and automated image-based measurement of contact angle, contact length, and deformation.

Acknowledgments

The research work was funded by Austria Wirtschaftsservice Gesellschaft mbH (aws) within the framework of Proof-of-Concept, project number P2505626.

References

1. Bendsøe, M.P., Sigmund, O.: Topology optimization. In: Optimization of Structural and mechanical systems, pp. 161–194. World Scientific (2007). https://doi.org/10.1142/6214
2. Crooks, W., Vukasin, G., O'Sullivan, M., Messner, W., Rogers, C.: Fin ray® effect inspired soft robotic gripper: From the robosoft grand challenge toward optimization. Frontiers in Robotics and AI **3**, 70 (2016). https://doi.org/10.3389/frobt.2016.00070
3. Hughes, J., Culha, U., Giardina, F., Guenther, F., Rosendo, A., Iida, F.: Soft manipulators and grippers: A review. Frontiers in Robotics and AI **3**, 69 (2016). https://doi.org/10.3389/frobt.2016.00069
4. Kim, S., Laschi, C., Trimmer, B.: Soft robotics: a bioinspired evolution in robotics. Trends in Biotechnology **31**(5), 287–294 (2013). https://doi.org/10.1016/j.tibtech.2013.03.002
5. Liu, C.H., Shih, Y.C., Chi, J.C.: Topology optimization and prototype of a highly adaptive multi-material compliant finger for parallel grippers. IEEE Robotics and Automation Letters **9**(9), 8067–8074 (2024). https://doi.org/10.1109/LRA.2024.3440837
6. Pfeifer, R., Lungarella, M., Iida, F.: The challenges ahead for bio-inspired'soft'robotics. Communications of the ACM **55**(11), 76–87 (2012). https://doi.org/10.1145/2366316.236633
7. Rus, D., Tolley, M.T.: Design, fabrication and control of soft robots. Nature **521**(7553), 467–475 (2015). https://doi.org/10.1038/nature14543
8. Shan, X., Birglen, L.: Modeling and analysis of soft robotic fingers using the fin ray effect. The International Journal of Robotics Research **39**(14), 1686–1705 (2020). https://doi.org/10.1177/0278364920913926
9. Shintake, J., Cacucciolo, V., Floreano, D., Shea, H.: Soft robotic grippers. Advanced Materials **30**(29), 1707035 (2018). https://doi.org/10.1002/adma.201707035
10. Sigmund, O.: On the design of compliant mechanisms using topology optimization. Mechanics of Structures and Machines **25**(4), 493–524 (1997). https://doi.org/10.1080/08905459708945415
11. Srinivas, G.L., Alshawabkeh, M., Brandstötter, M.: Design and development of fin-ray finger using topology optimization with multiple load cases. In: 2024 International Conference on Cognitive Robotics and Intelligent Systems (ICC-ROBINS). pp. 1–7. IEEE (2024). https://doi.org/10.1109/ICC-ROBINS60238.2024.10534011
12. Srinivas, G.L., Javed, A., Faller, L.M.: Versatile 3D-printed fin-ray effect soft robotic fingers: lightweight optimization and performance analysis. Journal of the Brazilian Society of Mechanical Sciences and Engineering **46**(6), 382 (2024). https://doi.org/10.1007/s40430-024-04957-0

13. Suder, J., Bobovský, Z., Mlotek, J., Vocetka, M., Oščádal, P., Zeman, Z.: Structural optimization method of a finray finger for the best wrapping of object. Applied Sciences **11**(9), 3858 (2021). https://doi.org/10.3390/app11093858
14. Trivedi, D., Rahn, C.D., Kier, W.M., Walker, I.D.: Soft robotics: Biological inspiration, state of the art, and future research. Applied Bionics and Biomechanics **5**(3), 99–117 (2008). https://doi.org/10.1080/11762320802557865
15. Yang, Y., Jin, K., Zhu, H., Song, G., Lu, H., Kang, L.: A 3d-printed fin ray effect inspired soft robotic gripper with force feedback. Micromachines **12**(10), 1141 (2021). https://doi.org/10.3390/mi12101141
16. Yao, J., Fang, Y., Yang, X., Wang, P., Li, L.: Design optimization of soft robotic fingers biologically inspired by the fin ray effect with intrinsic force sensing. Mechanism and Machine Theory **191**, 105472 (2024). https://doi.org/10.1016/j.mechmachtheory.2023.105472
17. Zhu, B., Zhang, X., Zhang, H., Liang, J., Zang, H., Li, H., Wang, R.: Design of compliant mechanisms using continuum topology optimization: A review. Mechanism and Machine Theory **143**, 103622 (2020). https://doi.org/10.1016/j.mechmachtheory.2019.103622